J Neurophysiol 110: 2312–2324, 2013.
First published August 21, 2013; doi:10.1152/jn.00137.2013.

Unmasking the obligatory components of nociceptive event-related brain potentials

A. Mouraux,[1] A. L. De Paepe,[2] E. Marot,[1] L. Plaghki,[1] G. D. Iannetti,[3] and V. Legrain[1,2]
[1]*Institute of Neuroscience (IoNS), Université catholique de Louvain, Brussels, Belgium;* [2]*Department of Experimental Clinical and Health Psychology, Ghent University, Ghent, Belgium; and* [3]*Department of Neuroscience, Physiology, and Pharmacology, University College London, London, United Kingdom*

Submitted 26 February 2013; accepted in final form 19 August 2013

Mouraux A, De Paepe AL, Marot E, Plaghki L, Iannetti GD, Legrain V. Unmasking the obligatory components of nociceptive event-related brain potentials. *J Neurophysiol* 110: 2312–2324, 2013. First published August 21, 2013; doi:10.1152/jn.00137.2013.—It has been hypothesized that the human cortical responses to nociceptive and nonnociceptive somatosensory inputs differ. Supporting this view, somatosensory-evoked potentials (SEPs) elicited by thermal nociceptive stimuli have been suggested to originate from areas 1 and 2 of the contralateral primary somatosensory (S1), operculo-insular, and cingulate cortices, whereas the early components of nonnociceptive SEPs mainly originate from area 3b of S1. However, to avoid producing a burn lesion, and sensitize or fatigue nociceptors, thermonociceptive SEPs are typically obtained by delivering a small number of stimuli with a large and variable interstimulus interval (ISI). In contrast, the early components of nonnociceptive SEPs are usually obtained by applying many stimuli at a rapid rate. Hence, previously reported differences between nociceptive and nonnociceptive SEPs could be due to differences in signal-to-noise ratio and/or differences in the contribution of cognitive processes related, for example, to arousal and attention. Here, using intraepidermal electrical stimulation to selectively activate Aδ-nociceptors at a fast and constant 1-s ISI, we found that the nociceptive SEPs obtained with a long ISI are no longer identified, indicating that these responses are not obligatory for nociception. Furthermore, using a blind source separation, we found that, unlike the obligatory components of nonnociceptive SEPs, the obligatory components of nociceptive SEPs do not receive a significant contribution from a contralateral source possibly originating from S1. Instead, they were best explained by sources compatible with bilateral operculo-insular and/or cingulate locations. Taken together, our results indicate that the obligatory components of nociceptive and nonnociceptive SEPs are fundamentally different.

pain; nociception; event-related potentials; primary somatosensory cortex; laser-evoked potentials; intraepidermal stimulation

FOR THE PAST 30 YEARS, a large number of studies have aimed at understanding the neural mechanisms underlying the processing of nociceptive input and the perception of pain in the human cortex. Most of these studies have relied on noninvasive techniques to sample brain activity, such as electroencephalography (EEG), magnetoencephalography (MEG), functional magnetic resonance imaging (fMRI), and positron emission tomography (PET) (Bushnell and Apkarian 2005; Garcia-Larrea et al. 2003; Kakigi et al. 2005; Peyron et al. 2002; Treede et al. 1999). With these techniques, it has been shown repeatedly that nociceptive stimuli elicit responses in a wide array of brain areas, including postcentral, operculo-insular, and cingulate areas. A number of investigators have considered that the combined activation of these brain regions is responsible for the transformation of nociceptive input into a conscious perception of pain, in particular, the coding of pain intensity and pain unpleasantness (Boly et al. 2008; Brooks and Tracey 2005; Cheng et al. 2007; Ingvar 1999; Jones 1998; Moisset and Bouhassira 2007; Singer et al. 2004; Stern et al. 2006; Valeriani et al. 2008; Whyte 2008).

To identify distinctive features of the cortical processing of nociception and touch, several studies have compared the EEG responses elicited by the specific activation of nociceptive Aδ and C fibers vs. the selective activation of nonnociceptive Aβ fibers (Inui et al. 2003a; Kunde and Treede 1993; Ploner et al. 2000; Valeriani et al. 2004). These studies have suggested that one important difference may reside in the responses to nociceptive and nonnociceptive input within the primary somatosensory cortex (S1). Indeed, early-latency nonnociceptive somatosensory-evoked potentials (SEPs) elicited, for example, by the transcutaneous electrical activation of Aβ fibers, receive a strong contribution from activity originating from a tangential source located within area 3b of S1 contralateral to the stimulated side. This contribution is clearly responsible for the earliest identifiable peak in the obtained SEP waveforms (e.g., the N20 wave following stimulation of the median nerve) (Legatt and Kader 2000; Regan 1989). In contrast, although there is increasing evidence that S1 does contribute to nociceptive SEPs such as laser-evoked potentials (Schlereth et al. 2003; Tarkka and Treede 1993; Valentini et al. 2012), this contribution does not display the typical reversal of polarity over the central sulcus (Baumgartner et al. 2011; Frot et al. 2013; Kanda et al. 2000; Ohara et al. 2004a), suggesting that nociceptive and nonnociceptive somatosensory stimuli do not trigger responses within the same subregions of S1.

Another important difference between nociceptive and nonnociceptive SEPs is the strong dominance of activities culminating at the scalp vertex in nociceptive SEPs (Garcia-Larrea et al. 2003). Despite the fact that these vertex responses can be elicited by any kind of stimulus regardless of sensory modality (Mouraux and Iannetti 2009), their contribution to nociceptive SEPs is often considered to be more obligatory, and this has been hypothesized to reflect the particular engagement of the ACC and/or operculo-insular regions in pain perception. However, the contribution of these activities to all event-related brain potentials (ERPs), including those elicited by nociceptive stimuli, appears to depend greatly on the saliency of the elic-

Address for reprint requests and other correspondence: A. Mouraux, Institute of Neuroscience (IONS), Université catholique de Louvain, 53, Ave. Mounier—UCL B1.53.04, B-1200 Brussels, Belgium (e-mail: andre.mouraux@uclouvain.be).

iting stimulus and/or its relevance for the ongoing cognitive task (Iannetti et al. 2008; Legrain et al. 2012). Therefore, the dominant contribution of these vertex responses to nociceptive SEPs could reflect mainly the engagement of nonobligatory and modality-unspecific processes that depend on the environmental and cognitive context within which the stimulus appears (e.g., factors determining stimulus saliency) (Carmon et al. 1976; Davis 1939; Iannetti and Mouraux 2010; Legrain et al. 2011; Stowell 1984).

However, as already emphasized by Garcia-Larrea et al. (2003), the validity of the comparison between nociceptive and nonnociceptive SEPs is considerably undermined by the fact that the stimulation protocols typically used to elicit nociceptive SEPs are markedly different from the stimulation protocols typically used to disclose the early-latency components of nonnociceptive SEPs. To elicit nociceptive SEPs, it is usually recommended to use a small number of stimuli (e.g., 20–40 stimuli) applied with a long and variable interstimulus interval (ISI) (e.g., >6 s; Cruccu et al. 2008). This contrasts strongly with the large number of stimuli (e.g., 500–1,000 stimuli) and the short and constant ISI (e.g., 250 ms) that are most often used to disclose short-latency nonnociceptive SEPs (Cruccu et al. 2008). This difference is mainly due to the fact that the selective activation of nociceptors typically relies on thermal stimulators (such as infrared lasers or contact heat thermodes) that require to *1*) limit the total number of applied stimuli, *2*) use long ISIs, and *3*) displace the stimulus target between trials in order to avoid skin overheating, nociceptor habituation, and/or nociceptor sensitization (Plaghki and Mouraux 2003, 2005). Another important difference is that subjects are usually requested to respond to the nociceptive stimuli, for example, by rating the intensity of the elicited pain percept or performing a simple reaction time task.

All of these experimental factors are expected to increase the saliency and relevance of the stimuli and, thereby, inevitably enhance the contribution of nonobligatory and unspecific brain responses reflecting high-order cognitive functions such as attention (Legrain et al. 2012). Furthermore, because nociceptive SEPs are obtained by averaging a very limited number of trials, the previously reported differences between nociceptive SEPs and early-latency nonnociceptive SEPs could also be due to the lower signal-to-noise ratio (SNR) of the obtained SEP waveforms.

For these reasons, the failure of previous studies to identify early and obligatory brain responses to nociceptive stimulation could be mainly due to the fact that SEPs elicited by nociceptive stimuli have been examined in a context that *1*) maximizes the contribution of unspecific brain responses related to cognitive processing and *2*) precludes the identification of SEPs with a small amplitude. The objective of the present study was to test this hypothesis by delivering nociceptive stimuli in an experimental setting that allows the repetition of a large number of stimuli at a fast and constant rate. To achieve this goal, small electrical currents delivered through an intraepidermal needle electrode (Inui et al. 2002) were used to activate Aδ nociceptors selectively (Mouraux et al. 2010). Importantly, intraepidermal electrical stimulation (IES) activates nociceptive fibers directly. Hence, the afferent volley generated by IES may be expected to be more synchronous than the afferent volley generated by thermal stimulation, which requires transduction of the thermal stimulus into a neural impulse. Furthermore, IES can be applied with a high rate of stimulation and can be repeated a great number of times. Therefore, the use of IES allowed us to record, for the first time, high-SNR nociceptive SEPs and to perform a direct within-subject comparison of these responses to *1*) nonnociceptive SEPs elicited by transcutaneous electrical stimulation (TES) applied with the same experimental paradigm and *2*) nociceptive SEPs elicited by a small number of stimuli delivered with a long and variable ISI.

METHODS

Ethical Statement

Written informed consent was obtained from all participants. The study was approved by the local Ethics Committee of the Université catholique de Louvain and conformed to the latest revision of the Declaration of Helsinki.

Participants

Eighteen healthy volunteers took part in the study. Nine subjects participated in *experiment 1* (5 women, 4 men; all right-handed, aged 21–28 yr). Nine other subjects participated in *experiment 2* (4 women, 5 men; all right-handed, aged 21–35 yr). Both experiments were conducted in a dim, silent, temperature-controlled room. Participants lay semisupine in a comfortable armchair. Before each experiment, they were familiarized with the experimental setup and exposed to a small number of test stimuli applied to the left hand.

Experiment 1

Conventional TES was used to activate nonnociceptive Aβ fibers selectively. The stimuli were delivered to the median nerve through a pair of round felt-tip electrodes (Ø: 7 mm, interelectrode distance: 2.5 cm) soaked with electrolyte and applied against the skin at the wrist. Before each stimulation block, the intensity of the stimulus was set just above the motor threshold for thumb movement (Cruccu et al. 2008).

IES was used to activate Aδ nociceptors selectively. The stimuli were delivered to the hand dorsum with a stainless steel concentric bipolar electrode (Inui et al. 2002, 2006) consisting of a needle cathode (length: 0.1 mm, Ø: 0.2 mm) surrounded by a cylindrical anode (Ø: 1.4 mm). By gently pressing the device against the skin, the needle electrode was inserted in the superficial epidermis.

The intensity of stimulation is a crucial feature determining whether IES activates nociceptive free nerve endings selectively. Indeed, the selectivity of IES relies on the fact that cutaneous nociceptive free nerve endings are located more superficially than encapsulated Aβ fiber mechanoreceptors (Inui et al. 2002). Therefore, and as demonstrated in our previous study (Mouraux et al. 2010), if low intensities of stimulation are used, the very focal currents generated by IES activate nociceptive afferents without activating more deeply located low-threshold mechanoreceptors. However, if the intensity of stimulation is increased, the selectivity of IES is compromised because the stronger currents may also activate more deeply located Aβ fiber afferents. For this reason, Mouraux et al. (2010) found that IES delivered at twice the absolute detection threshold (0.08 ± 0.05 mA threshold averaged across the different experiments) only activates nociceptive afferents, whereas IES delivered at 2.5 mA also activates Aβ fibers. Similarly, de Tommaso et al. (2011) and Perchet et al. (2012) found that IES delivered above the threshold to elicit a sensation qualified as painful (e.g., 1.6 ± 0.5 mA; de Tommaso et al. 2011)—i.e., almost 10 times the absolute detection threshold—is not selective for nociceptors, as it elicits brain responses related to the activation of Aβ fibers.

The electrode was repositioned before each stimulation block, and the detection threshold ($P = 0.50$) to a single electrical pulse was estimated with a staircase procedure. The intensity of the stimulus used during the stimulation block was set to twice this detection threshold.

Because IES is thought to activate a very small number of afferents, several previous studies have proposed the use of short trains of stimulation to increase the strength of the nociceptive afferent volley through temporal summation and, thereby, to increase the SNR of the elicited responses. (Inui et al. 2006; Kaube et al. 2000). Importantly, because the intensity of the electrical current delivered during each pulse is not increased, the spatial distribution of the electrical current within the skin is not modified. For this reason, it has been postulated that increasing the number of pulses does not affect the selectivity of IES for nociceptive afferents, although repetition of the electrical pulse is likely to activate some additional fibers brought to a subthreshold potential by the preceding pulses. Therefore, in the present study, both TES and IES were delivered either as a single constant-current square-wave pulse lasting 0.5 ms (as in Mouraux et al. 2010) or as a train of three consecutive 0.5-ms pulses separated by a 5-ms interpulse interval (Fig. 1).

The stimuli or trains of stimuli were separated by a constant 1-s ISI. Each type of stimulus (single-pulse TES, 3-pulse TES, single-pulse IES, 3-pulse IES) was applied at the left and right hands in series of 400 trials (for each type of stimulus and for each hand location: 4 consecutive blocks of 100 stimuli, separated by a short-lasting rest period lasting 1–2 min). The order of the series was counterbalanced across participants. The entire experiment lasted ~2 h. At the end of each series, participants were asked to report the quality of the perception elicited by the stimulus by choosing one item within the following list of eight descriptors: "not perceived," "light touch," "touch," "shock," "tingling," "warm," "pricking," and "burning." This list of descriptors was used in several previous studies to compare the quality of the sensation elicited by nociceptive and tactile stimuli (Mouraux et al. 2010; Nahra and Plaghki 2003).

Electrophysiological recording. The EEG was recorded with 64 Ag-AgCl electrodes placed on the scalp according to the International 10-10 System (Waveguard64 cap, Cephalon). Scalp signals were recorded with an average reference. Ocular movements and eyeblinks were recorded with two additional bipolar surface electrodes placed at the upper left and lower right sides of the left eye. All signals were amplified and digitized at a 1,000-Hz sampling rate (64-channel ASA-LAB EEG system, Advanced Neuro Technologies).

Data analysis. All EEG processing steps were carried out with LetsWave 5 (http://amouraux.webnode.com/letswave) (Mouraux and Iannetti 2008), MATLAB (The MathWorks), and EEGLAB (http://sccn.ucsd.edu/eeglab).

Continuous EEG recordings were band-pass filtered (0.5–250 Hz) with a Butterworth zero-phase filter and segmented into 1-s-long epochs ranging from −0.25 to +0.75 s relative to stimulus onset. After baseline correction (reference interval −0.25 to 0 s), artifacts produced by eyeblinks or eye movements were subtracted with a validated method based on an independent component analysis (ICA) (Jung et al. 2000). In addition, epochs with amplitude values exceeding ±100 μV (i.e., epochs likely to be contaminated by an artifact) were rejected. These epochs constituted 6 ± 2% of the total number of epochs. Separate average waveforms were computed for each condition and participant.

To assess the group-level significance of the SEP waveforms obtained in the different conditions, a bootstrapping method was used to compare the signal amplitude within the poststimulus interval to the signal amplitude within the prestimulus interval (Delorme and Makeig 2004; Durka et al. 2004; Hu et al. 2012). To address the problem of multiple comparisons, the significance level was corrected by a false discovery rate (FDR) procedure (Durka et al. 2004). In addition, short-lasting epochs (<10 consecutive time bins) were discarded. See Hu et al. (2012) for additional details on this procedure.

Several distinct peaks were identified in all Aβ-SEP waveforms (N20, P30, N120, and P200) (Treede and Kunde 1995). For each subject and condition, the latency and baseline-to-peak amplitude of these peaks were extracted as follows: the N20 and P30 were identified at the central-parietal electrodes CP5 and CP6. The N120 was identified at the temporal electrodes T7 and T8. The P200 was identified at the vertex (electrode Cz). A single positive peak, referred to as P1, was consistently identified in the Aδ-SEP waveforms, whose latency and amplitude were measured at the vertex (electrode Cz), as the most positive value within the time interval ranging from 100 to 400 ms after stimulus onset.

Baseline-to-peak amplitudes and peak latencies obtained at each electrode were compared with a two-way repeated-measures ANOVA with stimulus location (left vs. right hand) and number of pulses (single vs. 3 pulses) as factors.

Blind source separation of SEPs related to activation of Aβ and Aδ fibers. For each participant, a blind source separation of SEPs related to the activation of Aβ (Aβ-SEPs) and Aδ (Aδ-SEPs) fibers was performed with an ICA (Makeig et al. 1997) constrained to an effective estimate of the intrinsic dimensionality of the original data (probabilistic ICA) (Beckmann and Smith 2004; Liang et al. 2010; Mouraux and Iannetti 2009). When applied to multichannel EEG recordings, ICA is a technique to separate independent sources linearly mixed in several sensors. Applied to scalp EEG, ICA separates the signals recorded on the scalp into a linear combination of independent components (ICs). Specifically, ICA optimizes a matrix W that linearly unmixes the multichannel EEG data X into a sum of temporally independent and spatially fixed components. The rows of the output matrix, $U = WX$, correspond to the time courses of the ICs, whereas the columns of the inverse matrix W^{-1} correspond to the relative projection strengths of the ICs at each scalp sensor. Each IC thus consists of a time course and a fixed scalp map. When ICA is unconstrained, the total number of ICs equals the total number of recording electrodes. Therefore, if the number of ICs differs greatly from the actual number of independent sources contributing to the

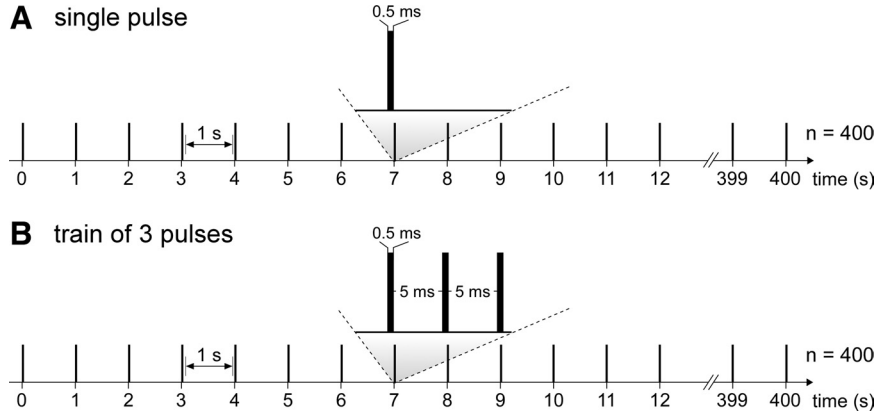

Fig. 1. In *experiment 1*, nociceptive and nonnociceptive somatosensory event-related potentials (SEPs) were elicited by electrical stimulation of the left and right hand. Intraepidermal electrical stimulation (IES) was used to selectively activate nociceptive Aδ fibers (Aδ-SEPs). Transcutaneous electrical stimulation (TES) of the median nerve at the wrist was used to selectively activate nonnociceptive Aβ fibers (Aβ-SEPs). The electrical stimuli were delivered either as a single constant-current square-wave pulse lasting 0.5 ms (*A*) or as a train of 3 consecutive 0.5-ms pulses separated by a 5-ms interpulse interval (*B*). Each type of stimulus (single pulse vs. train of 3 pulses; IES vs. TES; left vs. right hand) was repeated 400 times (4 separate blocks of 100 stimuli). All stimuli were separated by a constant 1-s interstimulus interval (ISI).

signal, this may constitute a critical problem (Beckmann and Smith 2004). Indeed, if the number of ICs is much greater than the number of sources, ICs containing spurious activity will appear because of overfitting. Conversely, if the number of ICs is much smaller than the number of sources, valuable information will be lost because of underfitting. The problem of overfitting could be particularly important when ICA is applied to averaged ERP waveforms, as the averaging procedure cancels out sources of activity unrelated to the stimulus, and hence the number of independent sources contributing to the average waveforms may be much smaller than the number of independent sources contributing to the original EEG signals. This fundamental limitation can be addressed with probabilistic ICA, a method that constrains the number of estimated ICs to an effective estimate of the number of independent sources contributing to the original data (Liang et al. 2010; Mouraux and Iannetti 2009). It is worth noting that the statistical independence between ICs does not imply that each IC necessarily reflects the activity generated by a single compact population of neurons (i.e., the activity of a single source). Indeed, if two or more spatially distinct populations of neurons are activated synchronously, their activity will not separate into distinct ICs. Nevertheless, the obtained IC will still reflect a functionally independent "network" of multiple sources (Delorme and Makeig 2004).

For each subject, the average waveforms of Aβ- and Aδ-SEPs elicited by single pulses and by trains of three pulses applied to the left and right hands were concatenated (8 average waveforms $\times$ 0.8 s $\times$ 1,000 Hz = 6,400 time points). Probabilistic ICA was then performed on this concatenated waveform in two steps: *1*) a probabilistic principal component analysis (PPCA) (Minka 2001) was used to decompose the multichannel concatenated average waveform into a number of principal components estimated by a method based on maximum likelihoods, operating on the eigenvalues of the principal component analysis (Rajan and Rayner 1997); and *2*) this subspace of principal components was rendered orthogonal with the Infomax ICA algorithm (Bell and Sejnowski 1995; Delorme and Makeig 2004), thus yielding a set of temporally independent ICs.

To estimate the contribution of each obtained IC to the different SEP waveforms, the time course of the power of each IC (μV^2) was expressed as the standard deviation from the mean (z scores) of the concatenated prestimulus intervals of all eight average waveforms (-0.25 to 0 s). z Scores were then averaged within the 0 to $+0.75$ s time interval following the onset of each stimulus, thus yielding eight values for each IC (1 value for each condition). If at least one of these eight values was greater than $z = 1.5$, the IC was considered to reflect stimulus-evoked EEG activity.

Source analysis and classification of ICs. The sources of each IC contributing significantly to the Aβ- and/or Aδ-SEP waveforms were estimated by fitting onto the IC scalp map a single dipole or a pair of dipoles with bilaterally symmetrical locations (assuming symmetrical activation of bilateral sources) with *dipfit2*, an algorithm based on a nonlinear optimization technique and a standardized boundary head element model (Fuchs et al. 2002; Woody 1967). First, fitting was attempted with a single-dipole model. If the residual variance exceeded 15%, fitting was attempted with a dipole pair constrained to symmetrical locations within the left and right hemispheres but not constrained to symmetrical orientations. If the residual variance still exceeded 15%, the IC was discarded. Given the limitations and inherent uncertainty of source analysis techniques, one can only speculate on the actual cortical generators of the different ICs. Nevertheless, on the basis of location and orientation of the obtained dipoles, it was possible to assign the majority of the modeled ICs to one of the following four categories: left hemisphere (1 single dipole located in the lateral aspect of the left hemisphere, i.e., $x < 20$ mm, Montreal Neurological Institute coordinate), right hemisphere (1 single dipole located in the lateral aspect of the right hemisphere, i.e., $x > 20$ mm), bilateral (1 pair of symmetrical dipoles located in the lateral aspect of the left and right hemispheres, i.e., $x > 20$ mm or $x < 20$ mm), and midline (1 single dipole located near the interhemispheric midline, i.e., $x > 20$ mm and $x < 20$ mm).

Average scalp maps were computed for each category of dipoles by averaging the scalp maps of all ICs belonging to the corresponding category. Because the absolute amplitude and polarity of these scalp maps are not meaningful (the polarity and amplitude of the back-projection at a given scalp channel and time point are dependent on both the sign and the strength of the channel weight and the sign and the weight of the IC time course), individual IC scalp maps were scaled such that the minimum and maximum values across channels equaled -1 and $+1$. Furthermore, polarities were arbitrarily defined as positive at electrode Fz.

Finally, time courses of the contribution of each category of ICs to each SEP waveform were obtained by back-projecting the selected category of ICs onto the scalp and computing the global field power of the reconstructed signals.

Experiment 2

Experiment 2 was performed to compare the Aδ-SEPs elicited by IES presented with a short and constant 1-s ISI (*experiment 1*) to the Aδ-SEPs elicited by IES presented with a long and randomly varying 5-to 10-s ISI (Fig. 2). The stimuli were applied only to the left hand dorsum, with trains of three constant-current square-wave electrical pulses with an ISI varying randomly from 5 to 10 s. As in *experiment 1*, the pulses lasted 0.5 ms and were separated by a 5-ms interpulse interval. The intensity of the stimulus was set to twice the detection threshold. The stimuli were delivered in four consecutive blocks of 10 trials. Each block was separated by a short-lasting rest period (2–5 min). The entire experiment lasted ~1 h.

In *experiment 2*, the EEG was recorded with 19 Ag-AgCl electrodes placed on the scalp according to the International 10-20 System. Ocular movements and eyeblinks were recorded with two additional bipolar surface electrodes placed at the upper left and lower right sides of the left eye. Signals were amplified, digitized at a 167-Hz sampling rate, and rereferenced with an average reference (PL-EEG, Walter Graphtek). N2 and P2 peak amplitudes and latencies were extracted at electrode Cz.

RESULTS

Experiment 1

Behavioral measures. The intensity of nonnociceptive TES was set to 2.33 $\pm$ 0.82 mA for single-pulse TES and 1.94 $\pm$ 0.51 mA for three-pulse TES at the left hand and to 2.33 $\pm$ 0.72 mA for single-pulse TES and 2.03 $\pm$ 0.40 mA for three-pulse TES at the right hand. The intensity of nociceptive IES was set to 0.20 $\pm$ 0.05 mA for single-pulse IES and 0.21 $\pm$ 0.07 mA for

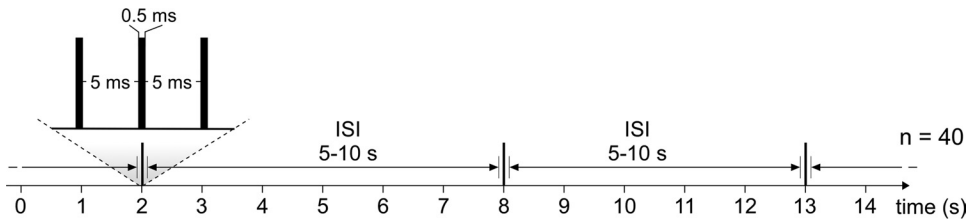

Fig. 2. In *experiment 2*, Aδ-SEPs were elicited by IES presented with a long and randomly varying ISI (40 stimuli; ISI = 5–10 s). IES was delivered to the left hand dorsum with trains of 3 consecutive 0.5-ms electrical pulses separated by a 5-ms interpulse interval.

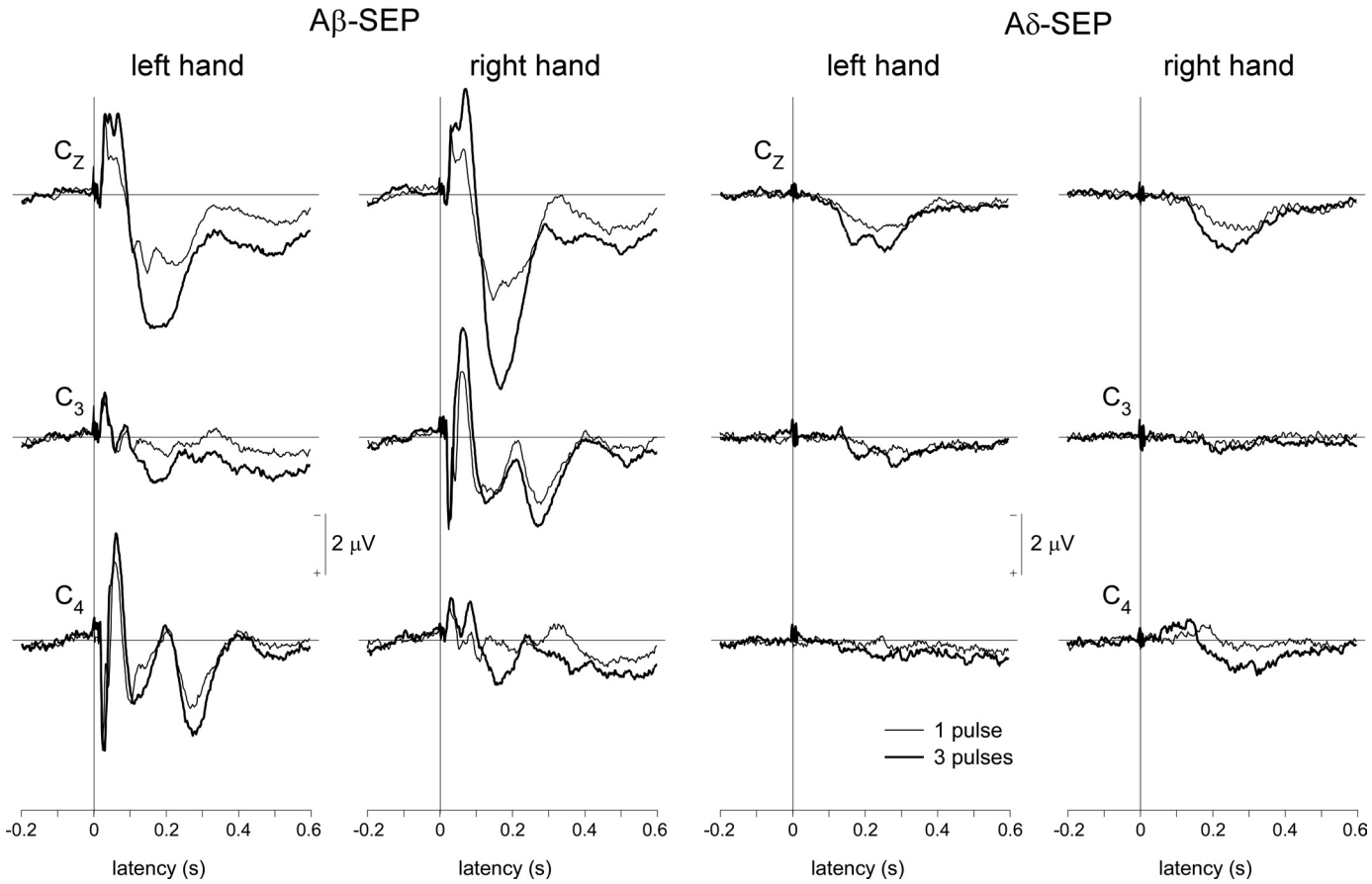

Fig. 3. *Experiment 1*. Group-level average of the SEPs elicited by stimulation of nonnociceptive Aβ fibers (Aβ-SEP; *left*) and nociceptive Aδ fibers (Aδ-SEP; *right*) obtained at electrodes Cz, C3, and C4 vs. an average reference. Each type of stimulus was repeated 400 times, separated by a constant 1-s ISI. The thin waveforms correspond to the Aβ- and Aδ-SEPs elicited by a single electrical pulse, whereas the thick waveforms correspond to the Aβ- and Aδ-SEPs elicited by a train of 3 consecutive pulses. *x*-Axis, time in seconds; *y*-axis, amplitude in microvolts.

three-pulse IES at the left hand and to 0.20 $\pm$ 0.06 mA for single-pulse IES and 0.22 $\pm$ 0.09 mA for three-pulse IES at the right hand. The intensities were not different according to the stimulus location and the number of pulses for both TES (all $F \leq$ 1.24, all $P \geq 0.298$) and IES (all $F \leq 1.93$, all $P \geq 0.203$).

When the stimulus consisted of a single pulse, nonnociceptive TES elicited a perception qualified as a "shock" by eight participants and qualified as "tingling" by one participant. When it consisted in a train of three pulses, the elicited percept was qualified as a "shock" (4 participants), as "tingling" (4 participants), and as "burning" (1 participant). In contrast, the percept elicited by nociceptive IES was qualified as "pricking" by eight of the nine participants and as "warm" by the remaining participant. When it consisted of three pulses, all nine participants qualified IES as "pricking."

During debriefing, participants reported that the intensity of the percept elicited by a single pulse of TES and by three pulses of TES remained constant throughout the stimulation block. In contrast, the intensity of the percept elicited by a single pulse of IES tended to fade, while the intensity of the percept elicited by three pulses of IES tended to remain more constant.

SEPs related to activation of Aβ fibers. In all subjects, nonnociceptive TES elicited clear Aβ-SEP waveforms, both when the stimulus consisted of a single pulse and when it consisted of a train of three pulses (Fig. 3, *left*). The first peak was identified ~20 ms after stimulus onset (Tables 1 and 2: N20). The N20 wave displayed a clearly lateralized scalp topography, appearing as a negative deflection over posterior parietal electrodes contralateral to the stimulated side and as a positive deflection over frontal electrodes (Fig. 4). Repeated-measures ANOVA revealed a significant effect of stimulus location on the magnitude of the N20 measured at electrodes CP5 ($F = 16.5$; $P = 0.004$) and CP6 ($F = 18.3$; $P = 0.003$). In contrast, the magnitude of the N20 was unaffected by the number of pulses factor, and there was no interaction between the two factors (Table 3).

Table 1. *Group-level average latency of nonnociceptive (Aβ) and nociceptive (Aδ) SEP components*

	Left		Right	
	1	3	1	3
Aβ-SEP				
N20	19 $\pm$ 1	19 $\pm$ 1	19 $\pm$ 1	18 $\pm$ 1
P30	33 $\pm$ 3	36 $\pm$ 7	33 $\pm$ 3	36 $\pm$ 5
N120	128 $\pm$ 18	121 $\pm$ 21	120 $\pm$ 16	122 $\pm$ 18
P200	180 $\pm$ 42	175 $\pm$ 29	181 $\pm$ 40	175 $\pm$ 28
Aδ-SEP				
P1	291 $\pm$ 37	254 $\pm$ 46	278 $\pm$ 68	236 $\pm$ 51

Values (in ms) are means $\pm$ SD for stimulation on right and left sides with 1 or 3 pulses. SEP, somatosensory-evoked potential.

Table 2. *Group-level average amplitude of nonnociceptive (Aβ) and nociceptive (Aδ) SEP components*

	Left		Right	
	1	3	1	3
Aβ-SEP				
N20				
CP5	−0.4 ± 0.4	−0.2 ± 0.4	−1.4 ± 0.8	−1.3 ± 1.0
CP6	−1.4 ± 1.0	−1.5 ± 1.0	−0.1 ± 0.3	−0.5 ± 0.6
P30				
CP5	0.0 ± 0.4	0.2 ± 0.6	4.4 ± 2.9	5.1 ± 2.4
CP6	4.8 ± 2.6	5.7 ± 2.7	0.3 ± 0.9	0.2 ± 1.2
N120				
T7	−2.2 ± 1.2	−2.2 ± 1.4	−4.1 ± 1.7	−5.0 ± 1.9
T8	−3.7 ± 1.9	−4.6 ± 2.8	−1.0 ± 0.9	−1.2 ± 1.5
P200				
Cz	3.5 ± 0.9	5.6 ± 2.2	4.4 ± 2.1	7.4 ± 3.5
Aδ-SEP				
P1				
Cz	1.6 ± 1.0	2.2 ± 1.2	1.6 ± 1.2	2.3 ± 1.3

Values (in μV) are means ± SD for stimulation on right and left sides with 1 or 3 pulses.

Like the scalp topography of the N20 wave, the later P30 and N120 waves (Fig. 3) displayed clearly lateralized scalp topographies that were dependent on stimulus location (Fig. 4). The P30 appeared as a positive deflection maximal over posterior parietal electrodes contralateral to the stimulated hand, while the N120 displayed a contralateral temporal maximum (Fig. 4). Repeated-measures ANOVA revealed a significant effect of stimulus location on the amplitude of the P30 measured at electrodes CP5 ($F = 33.0$; $P = 0.000$) and CP6 ($F = 52.0$; $P = 0.000$), as well as the N120 measured at electrodes T7 ($F = 47.8$; $P = 0.000$) and T8 ($F = 13.3$; $P = 0.007$). In contrast, the magnitude of the P30 and N120 waves was unaffected by the number of pulses, and there was no interaction between the two factors (Table 3).

In contrast to the preceding waves, the P200 displayed a symmetrical scalp distribution that was maximal at the vertex, independently of stimulus location (Fig. 4). Repeated-measures ANOVA showed that the amplitude of the P200 measured at Cz was not significantly modulated by the stimulus location ($F = 3.4$; $P = 0.102$) but was significantly modulated by the number of pulses ($F = 29.2$; $P = 0.001$). Indeed, the amplitude of the P200 wave was greater in response to three-pulse compared with single-pulse stimuli (Table 2). There was no significant interaction between the two factors ($F = 1.6$; $P = 0.244$).

The latencies of the N20, P30, N120, and P200 waves measured in the different experimental conditions (Table 1) were not significantly different.

SEPs related to activation of Aδ fibers. When the stimulus was delivered as a single pulse, nociceptive IES elicited a clearly identifiable Aδ-SEP waveform in only three of the nine participants. In contrast, when the stimulus was delivered as a train of three pulses, it elicited a clearly identifiable Aδ-SEP waveform in all participants (Figs. 3 and 5). Notably, the magnitude of this response was much smaller than that of the nonnociceptive SEP (Fig. 3). The obtained SEP waveforms could be summarized as a single positive deflection (P1), peaking 200–300 ms after stimulus onset (Tables 1 and 2). Regardless of the stimulated hand, the scalp topography of the P1 peak was maximal at the vertex and symmetrically distributed over both hemispheres (Fig. 5). The P1 peak elicited by a train of three pulses displayed a slightly more anterior scalp distribution (maximal over electrode Fz) than the P1 peak elicited by a single pulse. Repeated-measures ANOVA showed that the magnitude of the P1 (measured in all waveforms as the most positive value at electrode Cz within the time interval extending from 100 to 400 ms after stimulus onset) was not significantly modulated by stimulus location ($F = 0.1$; $P = 0.754$) but was significantly modulated by the number of pulses ($F = 17.9$; $P = 0.003$) (Table 3). The magnitude of the P1 wave was greater in response to three-pulse compared with single-pulse stimulation (Table 2). There was no interaction between the two factors ($F = 0.4$; $P = 0.557$). The latencies of the P1 peak measured in the different experimental conditions (Table 2) were not significantly different.

Results of the *t*-tests performed with each time point of the obtained Aδ-SEP waveforms are shown in Fig. 5. When nociceptive IES consisted of a single pulse, the Aδ-SEP waveforms were marginally significantly different from zero between ~250 and 500 ms after stimulus onset when stimulating the left and right hands. When nociceptive IES consisted of a train of three pulses, the Aδ-SEP waveforms were markedly significantly different from zero between ~160 and 600 ms after stimulus onset when stimulating the left and right hands. Notably, no significant deflection was found within the time interval compatible with the conduction velocity of Aβ fibers, i.e., before ~100 ms.

Blind source separation of Aβ- and Aδ-SEPs. On the basis of the estimate of the intrinsic dimensionality of the data, single-subject concatenated SEP waveforms were separated into 22.2 ± 4.5 ICs. Within these ICs, 8.7 ± 1.7 showed significant stimulus-evoked activity and 4.8 ± 2.0 were successfully modeled with the dipolar analysis.

On the basis of the location and orientation of the obtained dipoles (Fig. 6), the modeled ICs were assigned to one of the following four categories: left hemisphere (1.1 ± 0.9 ICs; mean ± SD), right hemisphere (1.9 ± 0.8 ICs), bilateral (1.1 ± 1.2 ICs), and midline (1.2 ± 0.9 ICs).

As shown in Fig. 6, ICs best modeled as a single dipole in the left hemisphere [residual variance (RV): 6.6 ± 2.4%] were, on average, located in the left central region and, most often, exhibited an anterior-posterior orientation relative to the scalp surface. The average scalp topography of these ICs displayed a negative maximum over the left parietal region, a polarity reversal over the left central region, and a positive maximum over frontal brain regions. Similarly, ICs best modeled as a single dipole in the right hemisphere (RV: 7.6 ± 3.2%) were clustered in the right central region and exhibited an anterior-posterior orientation relative to the scalp surface. The average scalp topography of these ICs displayed a negative maximum over the right parietal region, a polarity reversal over the right central region, and a positive maximum over frontal brain regions. These source locations and topographical distributions are similar to those of the early N20 wave elicited by median nerve TES and suggestive of activity originating from the left and right S1, respectively. ICs best modeled as a symmetrical pair of dipoles (RV: 5.6 ± 2.2%) tended to have a more caudo-cranial orientation, contrasting with the anterior-posterior orientation of the ICs modeled as a single dipole in the left or right hemisphere and compatible with activity originating

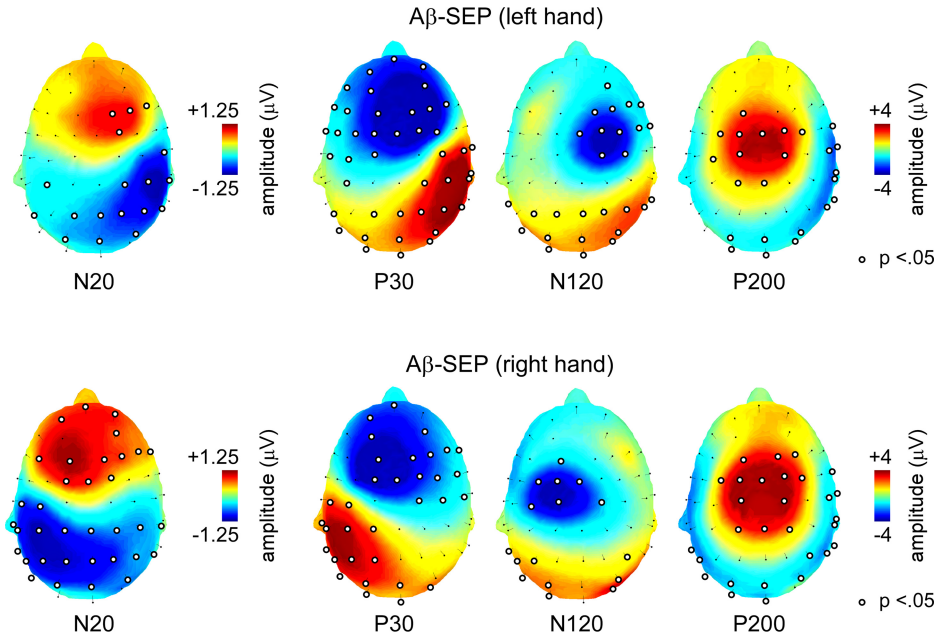

Fig. 4. *Experiment 1*. Group-level scalp topography of the N20, P30, N120, and P200 peaks of Aβ-SEPs elicited by TES of the left (*top*) and right (*bottom*) median nerve (train of 3 consecutive pulses separated by a 5-ms interpulse interval). For each subject and stimulation site, 400 stimuli were delivered with a constant 1-s ISI. The electrode locations where the group-level signal amplitude deviated significantly from baseline are marked by a black and white disk (1-sample *t*-test against zero; $P < 0.05$).

bilaterally from operculo-insular regions. The average scalp topography of these ICs was symmetrically distributed over both hemispheres and maximal over central-parietal regions (electrodes Cz and Pz). Finally, ICs best modeled as a single midline dipole (RV: 5.7 ± 2.6%) displayed a radial orientation and were clustered at a location compatible with activity originating from the cingulate cortex. Their scalp topography was symmetrical and maximal over frontal-central regions.

As shown in Fig. 7, left hemisphere ICs were the main contributors to the early part of the Aβ-SEPs elicited by stimulation of the right hand but did not contribute to the Aβ-SEPs elicited by stimulation of the left hand or to the Aδ-SEPs elicited by stimulation of the left or right hand. Similarly, right hemisphere ICs contributed almost exclusively to the early part of the Aβ-SEPs elicited by stimulation of the left hand. In contrast, ICs modeled as a symmetrical pair of dipoles in the left and right hemispheres (bilateral ICs) and midline ICs contributed predominantly to the later part of the Aβ-SEP waveforms and, most importantly, explained most of the Aδ-SEP waveform.

Experiment 2. Aδ-SEPs Elicited by Stimuli Presented with Long and Variable Interstimulus Interval

In all participants, IES applied with a long and variable 5- to 10-s ISI elicited Aδ-SEPs of much greater magnitude than the Aδ-SEPs elicited by stimuli applied with a constant 1-s ISI (Fig. 8).

Within the obtained average waveforms, two distinct peaks were identified (N2 and P2; Fig. 8). The N2 appeared as a negative deflection, peaking ~200 ms after stimulus onset, maximal at the vertex (Cz), and extending symmetrically toward left and right temporal electrodes (electrodes T7 and T8). The P2 appeared as a positive deflection, peaking ~350 ms after stimulus onset. It was also maximal at the vertex but did not extend toward lateral temporal electrodes. Although the scalp topography of the P2 shared some similarities with the

Table 3. *Effect of stimulated side and number of pulses on magnitude of nonnociceptive (Aβ) and nociceptive (Aδ) SEP components*

	Stimulated Side (*A*)		Number of Pulses (*B*)		*A* × *B*	
	F	*P* value	*F*	*P* value	*F*	*P* value
Aβ-SEP						
N20						
CP5	16.5	0.004*	1.2	*0.301*	0.6	*0.467*
CP6	18.3	0.003*	3.0	*0.120*	1.1	*0.318*
P30						
CP5	33.0	0.000*	4.4	*0.071*	2.3	*0.165*
CP6	52.0	0.000*	4.3	*0.073*	3.9	*0.083*
N120						
T7	47.8	0.000*	2.1	*0.188*	2.4	*0.162*
T8	13.3	0.007*	3.3	*0.107*	1.9	*0.202*
P200						
Cz	3.4	*0.102*	29.2	0.001*	1.6	*0.244*
Aδ-SEP						
P1						
Cz	0.1	*0.754*	17.9	0.003*	0.4	*0.557*

Values show effect of stimulated side (left vs. right hand) and number of pulses (1 pulse vs. 3 pulses) on magnitude of nonnociceptive (Aβ) and nociceptive (Aδ) SEP components. *$P < 0.01$. Nonsignificant *P* values are in italics.

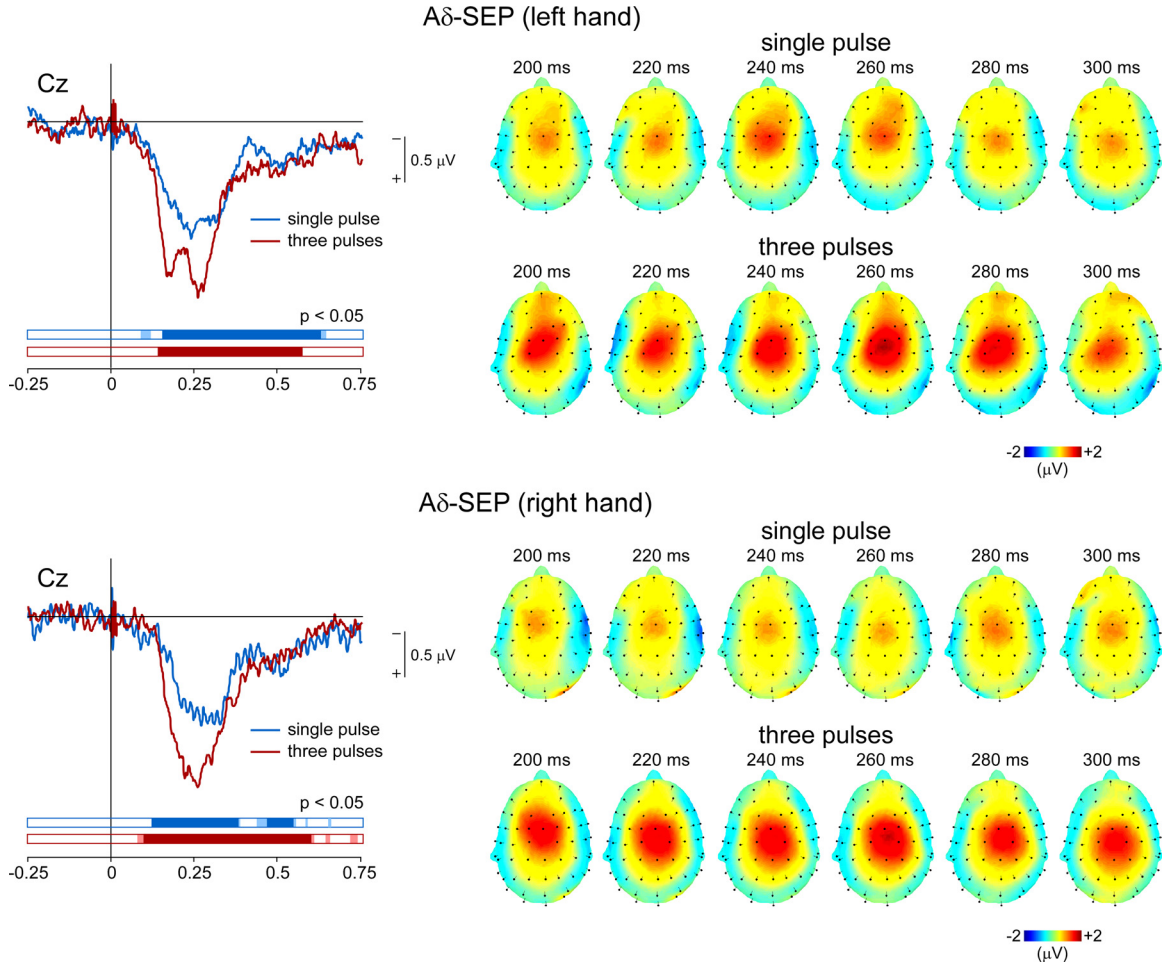

Fig. 5. *Experiment 1. Left*: group-level average waveforms (electrode Cz) and scalp topographies of nociceptive Aδ-SEPs elicited by IES of the left and right hand dorsum (blue waveforms, single pulse; red waveforms: 3 consecutive pulses delivered with a 5-ms interpulse interval). For each subject and stimulation site, 400 stimuli were delivered with a constant 1-s ISI. The elicited responses consisted of a positive deflection maximal at electrode Cz. To assess the group-level significance of this positive deflection, a bootstrapping method was used to compare the signal amplitude within the poststimulus interval to the signal amplitude within the prestimulus interval. To address the problem of multiple comparisons, the significance level was corrected with a false discovery rate (FDR) procedure (see METHODS). In addition, short-lasting epochs (<10 consecutive time bins) were discarded. The time intervals where the Aδ-SEP elicited by a single pulse deviated significantly from baseline are shown in light ($P < 0.05$) and dark ($P < 0.01$) blue. The time intervals where the Aδ-SEP elicited by a train of 3 pulses deviated significantly from baseline are shown in light ($P < 0.05$) and dark ($P < 0.01$) red. *Right*: to assess the scalp topography of this deflection, 6 group-level average scalp maps were computed at latencies ranging from 200 to 300 ms after stimulus onset.

scalp topography of the P1 of the Aδ-SEP elicited by stimulation with a constant 1-s ISI, its latency was significantly different ($\Delta T = 154 \pm 26$ ms, $t = 5.9$, $P < 0.0001$), thus indicating that these two peaks reflect distinct stimulus-evoked cortical responses.

DISCUSSION

The present study shows that nociceptive (Aδ) SEPs obtained by averaging the EEG response to 400 nociceptive stimuli applied with an intraepidermal electrode and delivered at short and constant ISIs of 1 s consist mainly of a single positive deflection (P1), peaking ~200 ms after the onset of the stimulus and symmetrically distributed over the scalp vertex. This was markedly different from the nonnociceptive (Aβ) SEPs obtained with the same stimulation parameters, which *1*) were of much greater amplitude and *2*) consisted of a series of successive deflections starting ~20 ms after the onset of the stimulus and *3*) whose early components (N20 and P30 waves) displayed a clearly lateralized scalp topography, maximal over the parietal region contralateral to the stimulated side.

Contribution of S1 to Nociceptive and Nonnociceptive SEPs

As expected, the scalp topographies of the early-latency components of the Aβ-SEP waveforms (N20 and P30 waves) were maximal over the parietal region contralateral to the stimulated side and displayed a reversal of polarity over central regions, compatible with an anterior-posterior source located in the S1 area contralateral to the stimulated side. In contrast, the Aδ-SEP waveform consisted of a single positive peak maximal at the scalp vertex and symmetrically distributed over both hemispheres, without any hint of a lateralized response. Because EEG captures only a fraction of the cortical activity elicited by a sensory stimulus, the present results do not rule out activation of S1 by IES. Nevertheless, the present results indicate that the obligatory components of nonnociceptive and nociceptive somatosensory SEPs are fundamentally different.

This difference was confirmed by applying a blind source separation technique combined with dipolar source modeling to the Aδ- and Aβ-SEP waveforms. Indeed, the ICs capturing

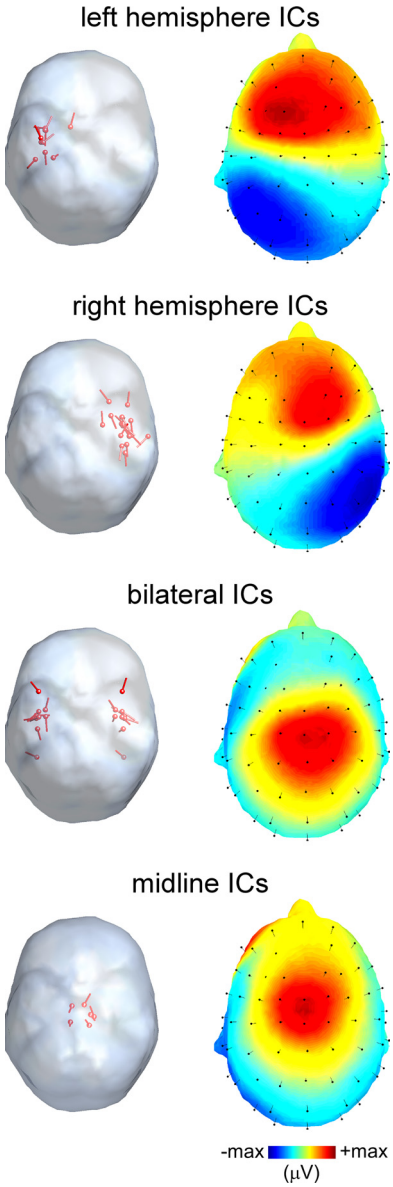

Fig. 6. *Experiment 1*. For each subject, a blind source separation of the concatenated Aβ- and Aδ-SEP average waveforms was performed using a probabilistic independent component analysis (PICA; see METHODS). The sources of each independent component (IC) contributing significantly to the Aβ-SEP and/or Aδ-SEP waveforms were then estimated by fitting a single dipole or a pair of dipoles with bilaterally symmetrical locations. On the basis of the location of the obtained dipoles, it was possible to assign each individual IC to one of the following 4 categories: left hemisphere, right hemisphere, bilateral, and midline. The glass brains show the location and orientation of each single dipole or dipole pair. Note that the polarity of the dipole moments (i.e., the direction of each dipole) is meaningless, because the polarity of the back-projection of each IC at a given scalp channel and time point is dependent on both the sign of the scalp channel weight and the sign of the IC time course. The scalp maps display the average topography of the ICs belonging to a given category (see METHODS).

the lateralized source of activity explaining most of the early part of the Aβ-SEP waveform did not contribute at all to the Aδ-SEP waveform (Fig. 7). The analysis also showed that later components of the Aβ-SEP waveform could be explained by the contribution of activity also contributing to most of the Aδ-SEP waveform. Source analysis of the scalp topography of these activities suggested sources compatible with activity originating from the left and right opercular-insular region as well as from a midline brain structure such as the cingulate cortex. Future studies using other techniques such as the intracranial recording of local field potentials are required to confirm the location of these sources, and to better understand the functional significance of nociception-related activity within these brain structures. For example, considering the function of nociception and the intrinsic saliency of nociceptive input, it could well be that these responses are mainly related to the detection and/or reaction to potentially meaningful stimuli in the sensory environment, such as physical threats. Taken together, these findings suggest that the obligatory stages of nociceptive and nonnociceptive somatosensory processing captured with ERPs differ significantly in that they do not elicit the same responses within S1.

This conclusion agrees with the results of several animal studies performed in monkeys. For example, studies performed with single-cell electrophysiology and optical neuroimaging have shown that in monkeys nonnociceptive tactile input is strongly represented in area 3b of the S1 cortex whereas nociceptive inputs are more strongly represented outside area 3b, such as in area 3a and/or area 1 of the S1 cortex (Kenshalo et al. 2000; Tommerdahl et al. 1996; Vierck et al. 2013; Whitsel et al. 2009). Furthermore, there is also evidence suggesting that an important difference between the thalamo-cortical projections of nociceptive and nonnociceptive somatosensory inputs in monkeys is that S1 is a main target for nonnociceptive somatosensory input but not for nociceptive somatosensory input. For example, with anterograde viral tracing, it was recently shown that that the bulk of nociceptive spino-thalamic input does not project to S1 but to the insular cortex, the secondary somatosensory cortex, and the cingulate cortex (Dum et al. 2009).

Contrasting with the present results, several studies using EEG and MEG have suggested that, in humans, the contralateral S1 area does contribute significantly to the ERPs and magnetic fields elicited by transient nociceptive stimuli (Inui et al. 2003a, 2003b; Kanda et al. 2000; Nakata et al. 2008; Ploner et al. 2000; Tarkka and Treede 1993; Timmermann et al. 2001; Valentini et al. 2012; Wang et al. 2007). Furthermore, studies relying on patient recordings obtained from subdural grids or implanted electrodes have also shown that thermal nociceptive stimuli elicit responses in the contralateral S1 area (Kanda et al. 2000; Ohara et al. 2004b). However, unlike the response to nonnociceptive vibro-tactile input, the S1 responses to nociceptive input do not show phase reversal across the central sulcus. This suggests that, as in monkeys (Kenshalo et al. 2000; Tommerdahl et al. 1996; Vierck et al. 2013; Whitsel et al. 2009), the S1 activity triggered by nociceptive input does not originate from a population of neurons whose orientation is predominantly anterior-posterior relative to the scalp surface (such as neurons in area 3b of the S1 cortex) and, instead, originates from a population of neurons whose orientation is largely radial to the scalp surface, such as neurons in area 3a and/or 1 of the S1 cortex.

However, these different arguments do not provide an explanation as to why the early components of the nociceptive SEPs elicited by stimuli delivered with a long and variable ISI exhibit a clearly lateralized scalp topography, maximal over the central and/or temporal region contralateral to the stimulated side (e.g., the N1 wave of laser-evoked potentials),

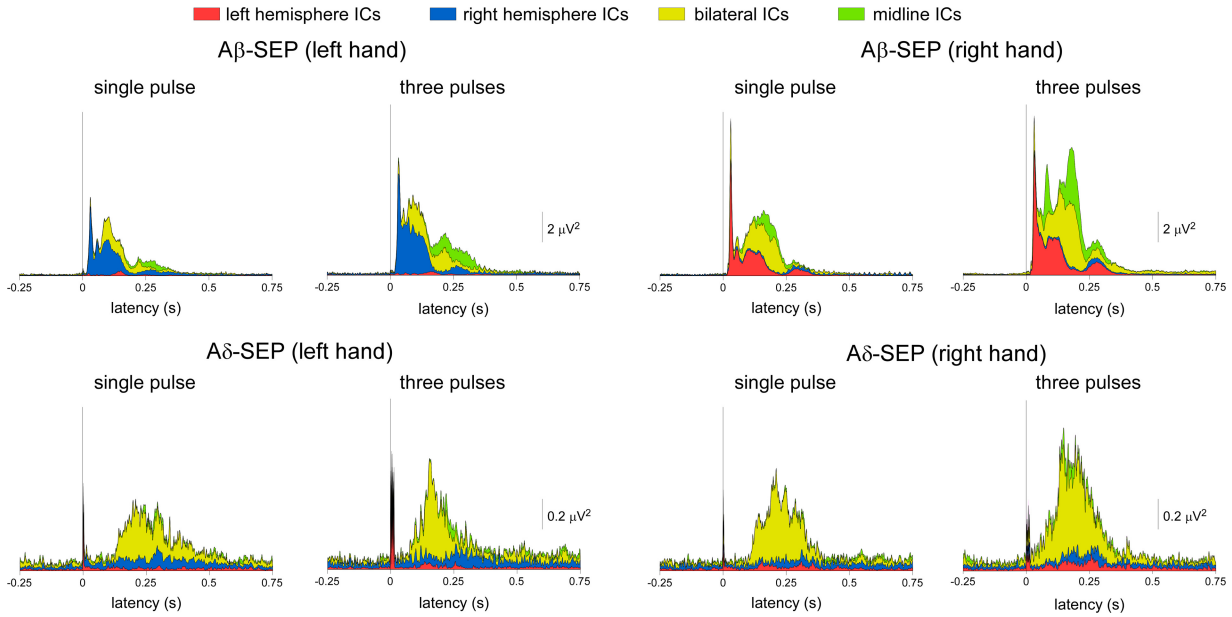

Fig. 7. *Experiment 1*. The cumulative contribution of left hemisphere (red), right hemisphere (blue), bilateral (yellow), and midline (green) ICs to the Aβ- and Aδ-SEP average waveforms was estimated by computing the global field power of the ICs back-projected onto the scalp. Note that the early-latency component of the Aβ-SEP waveform elicited by stimulation of the left hand is almost entirely explained by the contribution of right hemisphere ICs, whereas the early-latency component of the Aβ-SEP waveform elicited by stimulation of the right hand is almost entirely explained by the contribution of left hemisphere ICs (i.e., by ICs compatible with a tangential source in the contralateral S1). Also note that these ICs do not contribute to the Aδ-SEP waveforms, which, like the later part of the Aβ-SEP waveforms, are almost entirely explained by the contribution of bilateral ICs (i.e., ICs compatible with bilateral sources in operculo-insular cortices) and, to a lesser extent, midline ICs (i.e., ICs compatible with a source in the cingulate cortex).

whereas the nociceptive SEPs elicited by stimuli delivered with a short and constant ISI, as well as nociceptive steady-state evoked potentials (Colon et al. 2012; Mouraux et al. 2011), are symmetrically distributed over the two hemispheres. The lack of lateralized responses in short-ISI nociceptive SEPs and nociceptive steady-state evoked potentials suggests that these lateralized responses do not reflect cortical processes that are obligatory for nociception, i.e., that these lateralized responses are dependent on the context within which the stimulus is delivered. Supporting this view, it was very recently proposed that, unlike the responses to nonnociceptive somatosensory input, the responses to nociceptive input in area 3b of S1 are modified by light anesthesia as well as sustained stimulation (reviewed in Vierck et al. 2013), thus suggesting that these responses are dependent on context. Hence, the responses to nociceptive and nonnociceptive input in S1 could reflect functionally distinct processes, and such functional differences could explain the differential contribution of S1 to the responses elicited by nociceptive stimuli delivered at a rapid and constant rate.

Finally, the lack of S1 contribution to the Aδ-SEPs elicited by IES could be consequent to the fact that IES generates a very focal electrical field and hence that IES activates only very small number of afferent fibers compared with TES. This would explain the lower overall SNR of the EEG responses to IES compared with the EEG responses to TES. Furthermore, the afferent input generated by IES may be subject to peripheral habituation and/or may be less synchronized than the afferent input generated by TES. Therefore, a fraction of the EEG responses to IES could be canceled out by conventional time-domain averaging because it is not sufficiently time-locked to the onset of the stimulus. However, one would expect ERP components with a lower SNR to disappear before ERP components exhibiting a high SNR. Therefore, as the early-latency S1 contribution to the ERPs elicited by TES was much more prominent than all the contributions of other sources, it seems unlikely that an overall reduction in SNR could explain the lack of S1 contribution to the ERPs elicited by IES.

Effect of Temporal Summation on Nociceptive and Nonnociceptive SEPs

The number of electrical pulses used to generate the somatosensory stimulus (1 pulse vs. 3 consecutive pulses separated by a 5-ms interpulse interval) had no significant effect on the early-latency components of the Aβ-SEP waveform (i.e., the N20, P30, and N120 potentials), thus indicating that these peaks are mainly driven by the first-arriving input of the somatosensory volley, and that they reflect brain activity that does not significantly integrate the incoming somatosensory input over time.

In contrast, the number of electrical pulses significantly increased the magnitude of the later P200 potential of the Aβ-SEP waveform, as well as the P1 potential of the Aδ-SEP waveform, thus indicating that these potentials reflect brain activity whose magnitude is more strongly determined by temporal summation of the incoming somatosensory input. Importantly, the scalp topography and latency of the ERPs elicited by a single pulse of IES were highly similar to the scalp topography and latency of the ERPs elicited by a train of three pulses, indicating that both types of IES activated the same classes of afferents, i.e., nociceptive Aδ fibers as previously demonstrated in Mouraux et al. (2010).

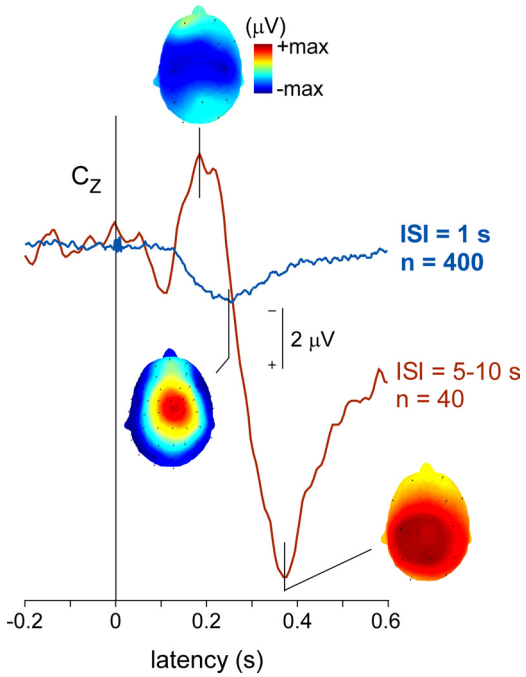

Fig. 8. *Experiment 2*. Comparison of the time course and scalp topography of the Aδ-SEPs elicited by IES of the left hand dorsum (3 electrical pulses separated by a 5-ms interpulse interval) with *1*) a constant 1-s ISI (blue waveform; group-level average; $n = 400$ trials per subject; *experiment 1*) and *2*) a variable ISI ranging between 5 and 10 s (red waveform; group-level average; $n = 40$ trials per subject; *experiment 2*). Signals are shown from electrode Cz vs. average reference. *x*-Axis, time in s, *y*-axis, amplitude in microvolts. The scalp maps represent the topography of the single positive peak obtained in *experiment 1* and the topography of the negative and positive peaks obtained in *experiment 2*.

Effect of Interstimulus Interval on Nociceptive SEPs

The Aδ-SEP obtained by averaging the EEG responses to 400 nociceptive stimuli applied with a constant 1-s ISI was markedly different from the Aδ-SEP obtained by averaging the EEG responses to 40 nociceptive stimuli applied with a variable 5- to 10-s ISI. Similar to what has been described in previous studies (Inui et al. 2003a; Mouraux et al. 2010), the Aδ-SEP elicited by nociceptive stimuli presented with a long and variable ISI consisted of a large negative-positive potential, labeled N2-P2, which was maximal at the scalp vertex, and whose shape and scalp topography resembled closely the shape and scalp topography of the N2-P2 complex of laser-evoked potentials. The amplitude of the N2-P2 elicited by IES applied with a variable 5- to 10-s ISI was more than one order of magnitude greater than the amplitude of the P1 wave elicited by IES applied with a constant 1-s ISI. Most importantly, the significant difference between the latency of the P1 wave identified in the Aδ-SEP elicited by stimuli presented with a 1-s ISI and the latency of the P2 wave identified in the Aδ-SEP elicited by stimuli presented with a long and variable ISI (~200 ms and ~350 ms, respectively) indicates that the two waves cannot be considered simply as scaled versions of the same underlying neural processes. Instead, the two waves most probably reflect temporally and functionally distinct cortical responses to nociceptive input.

The complete absence of the N2-P2 complex, as well as the complete absence of an early lateralized peak similar to the laser-evoked N1 wave, in the Aδ-SEP waveform elicited by stimuli presented with a constant 1-s ISI indicates that all these responses reflect brain processes that are not obligatory for nociception.

Furthermore, because IES applied at a constant 1-s ISI elicited a clear pinprick percept in all blocks (especially when delivered as a train of 3 pulses), the absence of the N1, N2, and P2 waves suggests that they reflect brain processes that are not required for the perception of nociceptive input. Whether the absence of these responses could be explained by refractoriness of nociceptive afferent pathways or cortical generators (Garcia-Larrea 2004) or by an interaction between Aδ fiber input and later-arriving C fiber input should be considered. However, these interpretations seem unlikely, as previous studies have shown that, even at ISIs as short as 250 ms, the magnitudes of laser-evoked N1, N2, and P2 waves are entirely unaffected by stimulus repetition when the ISI is varied randomly from trial to trial (Mouraux et al. 2004; Wang et al. 2010). Hence, it is likely that the occurrence of these responses is strongly dependent on contextual factors, such as factors that determine stimulus novelty (Iannetti et al. 2008; Legrain et al. 2011) and hence that these responses reflect brain processes mainly related to the detection and/or the reaction to salient sensory input.

However, it is important to note that the P1 wave elicited by stimulation at a constant 1-s ISI occurs at a later latency than the N1 and N2 waves elicited by stimulation with a long and variable ISI (Fig. 8). If one considers the classical view of sensory processing implying that sensory information is initially processed in unimodal sensory areas and then fed forward to multimodal areas for further higher-order sensory and cognitive processing, the former statement contradicts the hypothesis that the P1 wave reflects obligatory components of nociceptive processing whereas the N1 and N2 waves would reflect less specific cognitive processes. However, in other sensory modalities, several recent studies have suggested the existence of direct thalamocortical connections bypassing primary sensory cortices to provide a fast and efficient way for transmitting information from subcortical structures to multimodal cortical areas and thereby allow the early detection of and reaction to salient events (Liang et al. 2013). In such a view, the obligatory components of nociceptive processing reflected in the P1 wave should not necessarily occur before cortical activity related to the detection of saliency.

ACKNOWLEDGMENTS

We are grateful to Dr. K. Inui for providing us with a sample of intraepidermal stimulation electrodes. G. D. Iannetti is University Research Fellow of The Royal Society (UK).

GRANTS

V. Legrain and A. L. De Paepe are supported by Research Foundation Flanders (Belgium). A. Mouraux acknowledges support from the IASP Early Career Research Grant and from a Mandat d'Impulsion Scientifique of the Belgian FNRS.

DISCLOSURES

No conflicts of interest, financial or otherwise, are declared by the author(s).

AUTHOR CONTRIBUTIONS

Author contributions: A.M., A.L.D.P., E.M., L.P., G.D.I., and V.L. conception and design of research; A.M., A.L.D.P., E.M., and V.L. performed

experiments; A.M., A.L.D.P., E.M., L.P., and V.L. analyzed data; A.M., A.L.D.P., E.M., L.P., G.D.I., and V.L. interpreted results of experiments; A.M., G.D.I., and V.L. prepared figures; A.M., G.D.I., and V.L. drafted manuscript; A.M., L.P., G.D.I., and V.L. edited and revised manuscript; A.M., A.L.D.P., E.M., L.P., G.D.I., and V.L. approved final version of manuscript.

REFERENCES

Baumgartner U, Vogel H, Ohara S, Treede RD, Lenz F. Dipole source analyses of laser evoked potentials obtained from subdural grid recordings from primary somatic sensory cortex. *J Neurophysiol* 106: 722–730, 2011.

Beckmann CF, Smith SA. Probabilistic independent component analysis for functional magnetic resonance imaging. *IEEE Trans Med Imaging* 23: 137–152, 2004.

Bell AJ, Sejnowski TJ. An information-maximization approach to blind separation and blind deconvolution. *Neural Comput* 7: 1129–1159, 1995.

Boly M, Faymonville ME, Schnakers C, Peigneux P, Lambermont B, Phillips C, Lancellotti P, Luxen A, Lamy M, Moonen G, Maquet P, Laureys S. Perception of pain in the minimally conscious state with PET activation: an observational study. *Lancet Neurol* 7: 1013–1020, 2008.

Brooks J, Tracey I. From nociception to pain perception: imaging the spinal and supraspinal pathways. *J Anat* 207: 19–33, 2005.

Bushnell MC, Apkarian AV (Editors). *Textbook of Pain*. London: Churchill Livingstone, 2005, p. 267–289.

Carmon A, Mor J, Goldberg J. Evoked cerebral responses to noxious thermal stimuli in humans. *Exp Brain Res* 25: 103–107, 1976.

Cheng Y, Lin CP, Liu HL, Hsu YY, Lim KE, Hung D, Decety J. Expertise modulates the perception of pain in others. *Curr Biol* 17: 1708–1713, 2007.

Colon E, Nozaradan S, Legrain V, Mouraux A. Steady-state evoked potentials to tag specific components of nociceptive cortical processing. *Neuroimage* 60: 571–581, 2012.

Cruccu G, Aminoff MJ, Curio G, Guerit JM, Kakigi R, Mauguiere F, Rossini PM, Treede RD, Garcia-Larrea L. Recommendations for the clinical use of somatosensory-evoked potentials. *Clin Neurophysiol* 119: 1705–1719, 2008.

Davis PA. Effects of acoustic stimuli on the waking human. *J Neurophysiol* 2: 494–499, 1939.

de Tommaso M, Santostasi R, Devitofrancesco V, Franco G, Vecchio E, Delussi M, Livrea P, Katzarava Z. A comparative study of cortical responses evoked by transcutaneous electrical vs. CO_2 laser stimulation. *Clin Neurophysiol* 122: 2482–2487, 2011.

Delorme A, Makeig S. EEGLAB: an open source toolbox for analysis of single-trial EEG dynamics including independent component analysis. *J Neurosci Methods* 134: 9–21, 2004.

Dum RP, Levinthal DJ, Strick PL. The spinothalamic system targets motor and sensory areas in the cerebral cortex of monkeys. *J Neurosci* 29: 14223–14235, 2009.

Durka PJ, Zygierewicz J, Klekowicz H, Ginter J, Blinowska KJ. On the statistical significance of event-related EEG desynchronization and synchronization in the time-frequency plane. *IEEE Trans Biomed Eng* 51: 1167–1175, 2004.

Frot M, Magnin M, Mauguiere F, Garcia-Larrea L. Cortical representation of pain in primary sensory-motor areas (S1/M1)—a study using intracortical recordings in humans. *Hum Brain Mapp* 34: 2655–2668, 2013.

Fuchs M, Kastner J, Wagner M, Hawes S, Ebersole JS. A standardized boundary element method volume conductor model. *Clin Neurophysiol* 113: 702–712, 2002.

Garcia-Larrea L. Somatosensory volleys and cortical evoked potentials: "first come, first served"? *Pain* 112: 5–7, 2004.

Garcia-Larrea L, Frot M, Valeriani M. Brain generators of laser-evoked potentials: from dipoles to functional significance. *Neurophysiol Clin* 33: 279–292, 2003.

Hu L, Zhang ZG, Hu Y. A time-varying source connectivity approach to reveal human somatosensory information processing. *Neuroimage* 62: 217–228, 2012.

Iannetti GD, Hughes NP, Lee MC, Mouraux A. Determinants of laser-evoked EEG responses: pain perception or stimulus saliency? *J Neurophysiol* 100: 815–828, 2008.

Iannetti GD, Mouraux A. From the neuromatrix to the pain matrix (and back). *Exp Brain Res* 205: 1–12, 2010.

Ingvar M. Pain and functional imaging. *Philos Trans R Soc Lond B Biol Sci* 354: 1347–1358, 1999.

Inui K, Tran TD, Hoshiyama M, Kakigi R. Preferential stimulation of Adelta fibers by intra-epidermal needle electrode in humans. *Pain* 96: 247–252, 2002.

Inui K, Tran TD, Qiu Y, Wang X, Hoshiyama M, Kakigi R. A comparative magnetoencephalographic study of cortical activations evoked by noxious and innocuous somatosensory stimulations. *Neuroscience* 120: 235–248, 2003a.

Inui K, Tsuji T, Kakigi R. Temporal analysis of cortical mechanisms for pain relief by tactile stimuli in humans. *Cereb Cortex* 16: 355–365, 2006.

Inui K, Wang X, Qiu Y, Nguyen BT, Ojima S, Tamura Y, Nakata H, Wasaka T, Tran TD, Kakigi R. Pain processing within the primary somatosensory cortex in humans. *Eur J Neurosci* 18: 2859–2866, 2003b.

Jones A. The pain matrix and neuropathic pain. *Brain* 121: 783–784, 1998.

Jung TP, Makeig S, Humphries C, Lee TW, McKeown MJ, Iragui V, Sejnowski TJ. Removing electroencephalographic artifacts by blind source separation. *Psychophysiology* 37: 163–178, 2000.

Kakigi R, Inui K, Tamura Y. Electrophysiological studies on human pain perception. *Clin Neurophysiol* 116: 743–763, 2005.

Kanda M, Nagamine T, Ikeda A, Ohara S, Kunieda T, Fujiwara N, Yazawa S, Sawamoto N, Matsumoto R, Taki W, Shibasaki H. Primary somatosensory cortex is actively involved in pain processing in human. *Brain Res* 853: 282–289, 2000.

Kaube H, Katsarava Z, Kaufer T, Diener H, Ellrich J. A new method to increase nociception specificity of the human blink reflex. *Clin Neurophysiol* 111: 413–416, 2000.

Kenshalo DR, Iwata K, Sholas M, Thomas DA. Response properties and organization of nociceptive neurons in area 1 of monkey primary somatosensory cortex. *J Neurophysiol* 84: 719–729, 2000.

Kunde V, Treede RD. Topography of middle-latency somatosensory evoked potentials following painful laser stimuli and non-painful electrical stimuli. *Electroencephalogr Clin Neurophysiol* 88: 280–289, 1993.

Legatt AD, Kader A. Topography of the initial cortical component of the median nerve somatosensory evoked potential. Relationship to central sulcus anatomy. *J Clin Neurophysiol* 17: 321–325, 2000.

Legrain V, Iannetti GD, Plaghki L, Mouraux A. The pain matrix reloaded: a salience detection system for the body. *Prog Neurobiol* 93: 111–124, 2011.

Legrain V, Mancini F, Sambo CF, Torta DM, Ronga I, Valentini E. Cognitive aspects of nociception and pain: bridging neurophysiology with cognitive psychology. *Neurophysiol Clin* 42: 325–336, 2012.

Liang M, Mouraux A, Chan V, Blakemore C, Iannetti GD. Functional characterisation of sensory ERPs using probabilistic ICA: effect of stimulus modality and stimulus location. *Clin Neurophysiol* 121: 577–587, 2010.

Liang M, Mouraux A, Iannetti GD. Bypassing primary sensory cortices—a direct thalamocortical pathway for transmitting salient sensory information. *Cereb Cortex* 23: 1–11, 2013.

Makeig S, Jung TP, Bell AJ, Ghahremani D, Sejnowski TJ. Blind separation of auditory event-related brain responses into independent components. *Proc Natl Acad Sci USA* 94: 10979–10984, 1997.

Minka TP. Automatic choice of dimensionality for PCA. *Adv Neural Inform Process Syst* 13: 598–604, 2001.

Moisset X, Bouhassira D. Brain imaging of neuropathic pain. *Neuroimage* 37, *Suppl* 1: S80–S88, 2007.

Mouraux A, Guerit JM, Plaghki L. Refractoriness cannot explain why C-fiber laser-evoked brain potentials are recorded only if concomitant Adelta-fiber activation is avoided. *Pain* 112: 16–26, 2004.

Mouraux A, Iannetti GD. Across-trial averaging of event-related EEG responses and beyond. *Magn Reson Imaging* 26: 1041–1054, 2008.

Mouraux A, Iannetti GD. Nociceptive laser-evoked brain potentials do not reflect nociceptive-specific neural activity. *J Neurophysiol* 101: 3258–3269, 2009.

Mouraux A, Iannetti GD, Colon E, Nozaradan S, Legrain V, Plaghki L. Nociceptive steady-state evoked potentials elicited by rapid periodic thermal stimulation of cutaneous nociceptors. *J Neurosci* 31: 6079–6087, 2011.

Mouraux A, Iannetti GD, Plaghki L. Low intensity intra-epidermal electrical stimulation can activate Adelta-nociceptors selectively. *Pain* 150: 199–207, 2010.

Nahra H, Plaghki L. The effects of A-fiber pressure block on perception and neurophysiological correlates of brief non-painful and painful CO_2 laser stimuli in humans. *Eur J Pain* 7: 189–199, 2003.

Nakata H, Tamura Y, Sakamoto K, Akatsuka K, Hirai M, Inui K, Hoshiyama M, Saitoh Y, Yamamoto T, Katayama Y, Kakigi R. Evoked magnetic fields following noxious laser stimulation of the thigh in humans. *Neuroimage* 42: 858–868, 2008.

Ohara S, Crone NE, Weiss N, Treede RD, Lenz FA. Amplitudes of laser evoked potential recorded from primary somatosensory, parasylvian and medial frontal cortex are graded with stimulus intensity. *Pain* 110: 318–328, 2004a.

Ohara S, Crone NE, Weiss N, Treede RD, Lenz FA. Cutaneous painful laser stimuli evoke responses recorded directly from primary somatosensory cortex in awake humans. *J Neurophysiol* 91: 2734–2746, 2004b.

Perchet C, Frot M, Charmarty A, Flores C, Mazza S, Magnin M, Garcia-Larrea L. Do we activate specifically somatosensory thin fibres with the concentric planar electrode? A scalp and intracranial EEG study. *Pain* 153: 1244–1252, 2012.

Peyron R, Frot M, Schneider F, Garcia-Larrea L, Mertens P, Barral FG, Sindou M, Laurent B, Mauguiere F. Role of operculoinsular cortices in human pain processing: converging evidence from PET, fMRI, dipole modeling, and intracerebral recordings of evoked potentials. *Neuroimage* 17: 1336–1346, 2002.

Plaghki L, Mouraux A. How do we selectively activate skin nociceptors with a high power infrared laser? Physiology and biophysics of laser stimulation. *Neurophysiol Clin* 33: 269–277, 2003.

Plaghki L, Mouraux A. EEG and laser stimulation as tools for pain research. *Curr Opin Investig Drugs* 6: 58–64, 2005.

Ploner M, Schmitz F, Freund HJ, Schnitzler A. Differential organization of touch and pain in human primary somatosensory cortex. *J Neurophysiol* 83: 1770–1776, 2000.

Rajan JJ, Rayner PJ. Model order selection for the singular value decomposition and the discrete Karhunen-Loeve transform using a Bayesian approach. *IEE Proc Vision Image Signal Process* 144: 116–123, 1997.

Regan D. *Human Brain Electrophysiology: Evoked Potentials and Evoked Magnetic Fields in Science and Medicine*. New York: Elsevier, 1989.

Schlereth T, Baumgartner U, Magerl W, Stoeter P, Treede RD. Left-hemisphere dominance in early nociceptive processing in the human parasylvian cortex. *Neuroimage* 20: 441–454, 2003.

Singer T, Seymour B, O'Doherty J, Kaube H, Dolan RJ, Frith CD. Empathy for pain involves the affective but not sensory components of pain. *Science* 303: 1157–1162, 2004.

Stern J, Jeanmonod D, Sarnthein J. Persistent EEG overactivation in the cortical pain matrix of neurogenic pain patients. *Neuroimage* 31: 721–731, 2006.

Stowell H. Event related brain potentials and human pain: a first objective overview. *Int J Psychophysiol* 1: 137–151, 1984.

Tarkka IM, Treede RD. Equivalent electrical source analysis of pain-related somatosensory evoked potentials elicited by a CO_2 laser. *J Clin Neurophysiol* 10: 513–519, 1993.

Timmermann L, Ploner M, Haucke K, Schmitz F, Baltissen R, Schnitzler A. Differential coding of pain intensity in the human primary and secondary somatosensory cortex. *J Neurophysiol* 86: 1499–1503, 2001.

Tommerdahl M, Delemos KA, Vierck CJ Jr, Favorov OV, Whitsel BL. Anterior parietal cortical response to tactile and skin-heating stimuli applied to the same skin site. *J Neurophysiol* 75: 2662–2670, 1996.

Treede RD, Kenshalo DR, Gracely RH, Jones AK. The cortical representation of pain. *Pain* 79: 105–111, 1999.

Treede RD, Kunde V. Middle-latency somatosensory evoked potentials after stimulation of the radial and median nerves: component structure and scalp topography. *J Clin Neurophysiol* 12: 291–301, 1995.

Valentini E, Hu L, Chakrabarti B, Hu Y, Aglioti SM, Iannetti GD. The primary somatosensory cortex largely contributes to the early part of the cortical response elicited by nociceptive stimuli. *Neuroimage* 59: 1571–1581, 2012.

Valeriani M, Barba C, Le Pera D, Restuccia D, Colicchio G, Tonali P, Gagliardo O, Treede RD. Different neuronal contribution to N20 somatosensory evoked potential and to CO_2 laser evoked potentials: an intracerebral recording study. *Clin Neurophysiol* 115: 211–216, 2004.

Valeriani M, Betti V, Le Pera D, De Armas L, Miliucci R, Restuccia D, Avenanti A, Aglioti SM. Seeing the pain of others while being in pain: a laser-evoked potentials study. *Neuroimage* 40: 1419–1428, 2008.

Vierck CJ, Whitsel BL, Favorov OV, Brown AW, Tommerdahl M. Role of primary somatosensory cortex in the coding of pain. *Pain* 154: 334–344, 2013.

Wang AL, Mouraux A, Liang M, Iannetti GD. Stimulus novelty, and not neural refractoriness, explains the repetition suppression of laser-evoked potentials. *J Neurophysiol* 104: 2116–2124, 2010.

Wang X, Inui K, Kakigi R. Early cortical activities evoked by noxious stimulation in humans. *Exp Brain Res* 180: 481–489, 2007.

Whitsel BL, Favorov OV, Li Y, Quibrera M, Tommerdahl M. Area 3a neuron response to skin nociceptor afferent drive. *Cereb Cortex* 19: 349–366, 2009.

Whyte J. Clinical implications of the integrity of the pain matrix. *Lancet Neurol* 7: 979–980, 2008.

Woody C. Characterization of an adaptive filter for the analysis of variable latency neuroelectric signals. *Med Biol Eng* 5: 539–553, 1967.